

Water resistant nanopapers prepared by lactic acid modified cellulose nanofibers

Jatin Sethi¹, Muhammad Farooq¹, Sunanda Sain¹, Mohini Sain^{2,3},

Juho Antti Sirviö^{1*}, Mirja Ilikainen¹ and Kristiina Oksman^{1,2,3}

¹Fibre and Particle Engineering Research Unit, University of Oulu, Oulu, Finland.

²Division of Materials Science, Luleå University of Technology, Luleå, Sweden.

³Centre for Biocomposites and Biomaterials Processing, University of Toronto, Toronto, Canada.

*Corresponding author: Juho Antti Sirviö, Email: juho.sirvio@oulu.fi

Abstract

The current work reports a novel, completely water based approach to prepare the water resistant modified cellulose nanopapers. Lactic acid in aqueous medium was attached on cellulose nanofibers surface with the aid of ultra-sonication and later oligomerized (polymerized) by compression molding under high temperature and pressure, to obtain the modified nanopapers with enhanced mechanical properties. The modified nanopapers showed an increase of 32% in the elastic modulus and 30% in the yield strength over reference nanopapers. Additionally, the modified nanopaper was hydrophobic in nature and had superior storage modulus under moist conditions. The storage modulus of wet modified nanopaper was three times (2.4 GPa) compared to the reference nanopapers (0.8 GPa) after 1 hour immersion in water. Finally, the thermal stability of the modified nanopaper was also higher than reference nanopaper. The material reported is 100% bio-based.

Keywords: Cellulose Nanofibers, Lactic acid, Water resistant Nanopaper, Mechanical properties

1 Introduction

The growing human population and increasing consumption has resulted in excessive use of our non-renewable natural resources. This demands the development of new and more sustainable materials

24 from renewable resources. Cellulose, the most abundant renewable biomaterial in the world, has been
25 widely studied as a raw material for new biomaterials, especially as a form of nano-sized cellulose
26 crystals (CNCs) and fibers (CNFs). Nanocellulose has astonishing mechanical properties: an elastic
27 modulus of around 150 GPa (Lee et al. 2014) and for that reason it has widely been studied as
28 reinforcements for polymers (Lee et al. 2014), or as a sheet-like material termed as nanopaper (Sehaqui
29 et al. 2012).

30 Nanopapers are prepared by removing water from nanocellulose suspensions, usually by vacuum
31 filtration or evaporation. The morphology of the nanopapers indicate an intricate network of cellulose
32 nanofibers, which high amount of interfibrillar bonding due to presence of hydroxyl groups on
33 cellulose molecules. This bonding results in excellent mechanical properties; it has been demonstrated
34 that nanopapers can have modulus of 9.4-14 GPa and strength of 103-449 MPa (Lee et al.
35 2014)(Sehaqui et al. 2012). With such excellent properties and renewable nature, nanopapers have
36 raised themselves as potential replacement for non-renewable materials applications such as food
37 packaging and electronic displays (Sehaqui et al. 2014).

38 Despite high strength of the nanopapers, there exists a fundamental weakness: they lose their strength
39 in damp conditions. Sehaqui et al. portrays this problem in their work, they found that in wet state
40 tensile modulus of nanopapers was only 5% of the value in dry state (Sehaqui et al. 2014). Even in high
41 humidity of 95 %, the storage modulus was 25% of storage modulus in dry conditions. The reason
42 behind this was explained by the fact that in presence of water molecules, the interfibrillar bonds
43 between fibers are heavily weakened (Sehaqui et al. 2014). Due to absence of interfibrillar bond the
44 fibers easily slides under external stress resulting diminished strength to nanopaper. Additionally, water
45 molecules plasticizes the amorphous regions of cellulose (Benítez et al. 2013). This inability to combat
46 moisture negates the positive advantages of high strength nanopaper. Hence, it is of interest to prepare

47 the water resistant nanopapers. In fact, it has been proposed that commercial viability of nanopapers
48 can only be ensured if they have enhanced mechanical properties in the presence of water (absorbed
49 moisture or liquid) (Benítez et al. 2013).

50 The hydrophilicity of cellulose surface and its ability to absorb water can be altered by chemically
51 modifying the surface of nanocellulose. The functionalization of cellulose has been reported by using
52 two mechanisms: covalent grafting of chemical entities and physical adsorption on the cellulose surface
53 (Tingaut et al. 2012). Covalent grafting is a common approach to improve hydrophobicity of cellulose
54 nanofibrils. Sehaqui et al. prepared hydrophobic nanopapers by modifying cellulose by mild
55 esterification by alkyl chains, which showed decreased moisture intake (Sehaqui et al. 2014).
56 Additionally, the wet strength was improved as much as 24 times when compared to reference.
57 However, the esterification is usually done in organic solvent or monomer medium (Habibi 2014;
58 Sehaqui et al. 2014), which are hazardous and costly. Therefore, use of water as medium is of great
59 practical value.

60 This work uses esterification of CNF surface with lactic acid in water medium. Although, the
61 esterification of CNFs is not a vastly studied topic, few researchers have published relevant results in
62 solvent medium (Lönnberg et al. 2006)(Peltzer et al. 2014) (Teramoto et al. 2002). Esterification is a
63 dehydration reaction which is often is not feasible in water medium, as the reaction product itself is a
64 water molecule. The product water is in equilibrium with medium water and reaction is not preferred
65 due to law of mass action (Kobayashi et al. 1997). However, esterification in water medium has been
66 done with the help of catalysts. (Kobayashi et al. 1997) used lipase based enzyme for
67 polycondensation, and (Tanaka and Kurihashi 2003) used dodecylbenzenesulfonic acid as catalyst and
68 surfactant.

69 This work attempts a novel approach to prepare esterified CNF nanopapers, which includes the
70 ultrasonication of CNFs in presence of lactic acid in water medium. Chemical reactions with the aid of
71 acoustic energy relates to the field of sonochemistry. During sonication, cavities (vacuum pockets) are
72 formed which have short life time. The cavities implode at an extremely high speed to form hotspots
73 which have high temperatures and pressures, (5000 K and pressure of 1000 atmospheres). The process
74 is known as cavitation. Such extreme conditions can produce chemical reactions that may otherwise not
75 happen (Suslick 2000). After ultrasonication, modified nanopapers were made by removal of water
76 under vacuum filtration and further processing at high temperature (150 °C) and pressure (10 MPa).
77 The samples were characterized by tensile testing, swelling studies, dynamic mechanical analysis
78 (DMA) under varying moisture and thermogravimetric analysis (TGA).

79 **2 Experimental**

80 **2.1 Materials**

81 L-(+)-Lactic acid (80%) was purchased from Sigma-Aldrich. Stannous chloride (Merck Millipore) was
82 purchased from VWR. Bleached soft wood sulfite fibers were kindly supplied by Stora Enso (Oulu,
83 Finland). The pulp (1.6 wt. %) was grinded in Masuko grinder. The pulp was repeated fed in contact
84 mode from 0-point, and distance was gradually decreased from - 20 (3 passes), - 40 (4 passes), -60 (5
85 passes) and -90 (7 passes). The chemical composition of the reference pulp was 95.0 wt% cellulose, 4.2
86 wt% hemicellulose, 0.3 wt% lignin and 0.5 wt% inorganics.

87 **2.2 Modification of nanofibers and processing of nanopapers**

88 After the fibrillation, cellulose nanofibers were diluted to the concentration of 0.4 wt% and LA was
89 added according to formulation given in Table 1. It is worth mentioning that tests were conducted with
90 different level of LA, it was found that there is no significant effect on the properties of modified
91 nanopapers (especially modulus), perhaps due to the amount of LA attached to the surface of

92 nanocellulose was not different; therefore for the purpose of simplicity, only a relevant formulation is
 93 reported in this study. Stannous chloride was added in trace amounts as catalyst for esterification (Yoo
 94 et al. 2006). The suspensions were stirred at 9000 rpm in Ultra-turrax homogenizer for 5 minutes, and
 95 further sonicated with the help of probe type sonicator (Heilscher UP 400s). The sonication was
 96 stopped when the sonication energy reached 1100 J/ml. After the sonification the suspensions were
 97 kept in the oven at 100 °C for 36 hours. The schematics are presented in Figure 1. These suspensions,
 98 henceforth mentioned as LA modified CNFs, were used to make nanopapers.

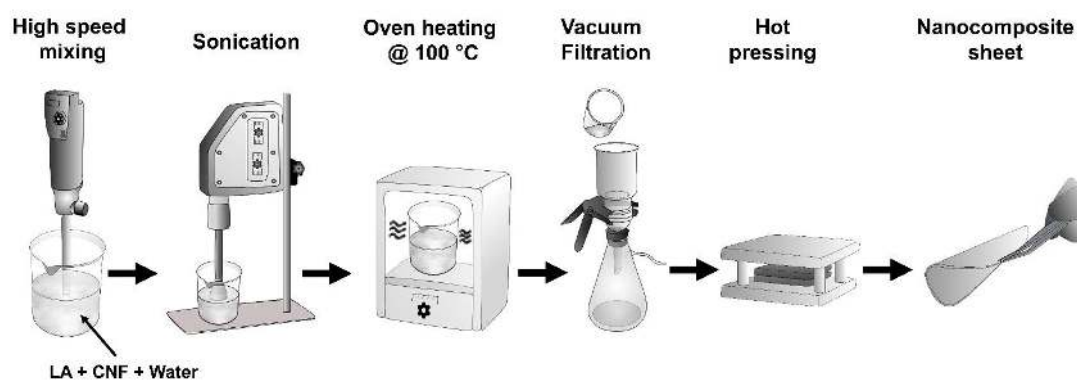
99 *Table 1 Formulations of CNF suspensions with lactic acid before sonication*

Sample name		
Materials	Reference nanopaper	Modified nanopaper
CNF	0.4	0.4
L-Lactic acid	0	7.6
SnCl ₂	0	0.0002
Water	99.6	92
Total	100 wt. %	100 wt. %

100

101 Nanopapers (reference and modified) were prepared by diluting LA modified CNFs and reference CNF
 102 suspension to 0.2 wt% by vacuum filtering through a Durapore PVDF membrane filter (Fisher
 103 Scientific, Pittsburgh, USA) with a pore size of 0.65 μm (Figure 1). The suspensions were degassed
 104 under the vacuum of 70 kPa for half an hour before the filtering. After the vacuum filtration, the wet
 105 cellulosic sheet was carefully peeled from the membrane and kept between two steel mesh cloths (mesh
 106 size 70 μm), which were further stacked in paper carrier board. The CNF sheet-steel mesh-paper board
 107 was kept under compression molding plates at temperature of 100 °C at the pressure of 10 MPa for 30

108 minutes to remove water. The LA-grafted nanopapers were further compression molded at 150°C for 5
 109 minutes, to increase the yield of esterification. In order to take account the effect of the sonication, two
 110 type of references were prepared, one sonicated suspension and one without sonication. All the
 111 nanopapers were stored in ambient conditions for 72 hours before testing. The grammage (weight in
 112 grams per square meters) of nanopapers was between 27-30 gsm.



113
 114 *Figure 1 Schematic diagram of process used for preparation of nanopapers*

115 2.3 Characterization

116 Diffuse reflectance infrared Fourier transform (DRIFT) spectroscopy was used to confirm the
 117 esterification of CNFs. The filtered wet cake from nanopaper preparation was rolled into a spherical
 118 shape and kept in oven at 90-95 °C overnight to remove water. The modified CNFs were further kept at
 119 150 °C for half an hour. It was done as because the restriction from the equipment that FTIR data from
 120 thin nanopapers was not feasible. The hardened reference and modified CNFs were grinded into
 121 powder, and the spectra were collected from dried samples with Bruker Vertex 80 V spectrometer
 122 (USA), in the 400–4000 cm^{-1} range, and 40 scans were taken at a resolution of 4 cm^{-1} for each
 123 sample.

124 Wide angle X-ray diffraction (WAXRD) was used to determine the crystalline structure of the
 125 reference and the modified nanopaper. Rigaku SmartLab 9kW rotating anode diffractometer (Japan)

126 using a Co K α radiation (40kV, 135 mA; $\lambda = 1.79030 \text{ \AA}$) was used for measurements. Bragg's angle
 127 (2θ) was varied from 10° to 50° , with a step width of 0.02° . The scanning speed was kept at 2° min^{-1} .
 128 The degree of crystallinity (CrI) was calculated from the peak intensity of the main crystalline plane
 129 (200) diffraction (I_{200}) which was at 26.2° and from peak intensity at 22° C, which is associated to
 130 amorphous fraction of cellulose (I_{am}) (French 2014), according to the Equation 1:

$$\text{CrI} = \left(\frac{I_{200} - I_{\text{am}}}{I_{200}} \right) \quad \text{Equation 1}$$

131 We would like to mention that due to the Co K α radiation source, the peak of cellulose have different
 132 diffraction angles compared to the peaks obtained for Cu K α radiation source.

133 The average size of crystallite (L) was calculated from the Scherrer equation (Ahtee et al. 1983) :

134

$$L = \frac{K \times \lambda}{\beta \times \cos\theta} \quad \text{Equation 2}$$

135

136 where K is a constant value 0.74, λ is the X-ray wavelength (0.17903 nm), β is the half-height width of
 137 the diffraction band (200); and θ is the Bragg angle corresponding to the (200) plane.

138 Mechanical testing was done to evaluate tensile properties of the CNF networks using Instron 5544

139 universal material testing machine (Norwood, USA). Strips with a length of 50 mm and a width of 5

140 mm were conditioned at 23°C and relative humidity (RH) of 50 % for 72 h prior to the testing. A load

141 cell of 100 N was used, the crosshead speed was 2 mm/min and the gauge length of 30 mm. The tests

142 were conducted in special chamber maintained at a RH 50 % and in the temperature of 23°C . The

143 elastic modulus (E) was determined from slope in linear region and yield strength $\sigma_{0.2}$ was determined

144 by intersection of 0.2% offset line and stress strain curve. The results are reported as average of
145 minimum 5 samples.

146 Zeiss Ultra Plus (Oberkochen, Germany) field emission scanning electron microscopy (FE-SEM) was
147 used for analysis of fiber-polymer network morphology of the samples. The acceleration voltage of 3
148 kV was used. The samples were coated with platinum to avoid charging. Inlens detector was used to
149 collect the signals for imaging.

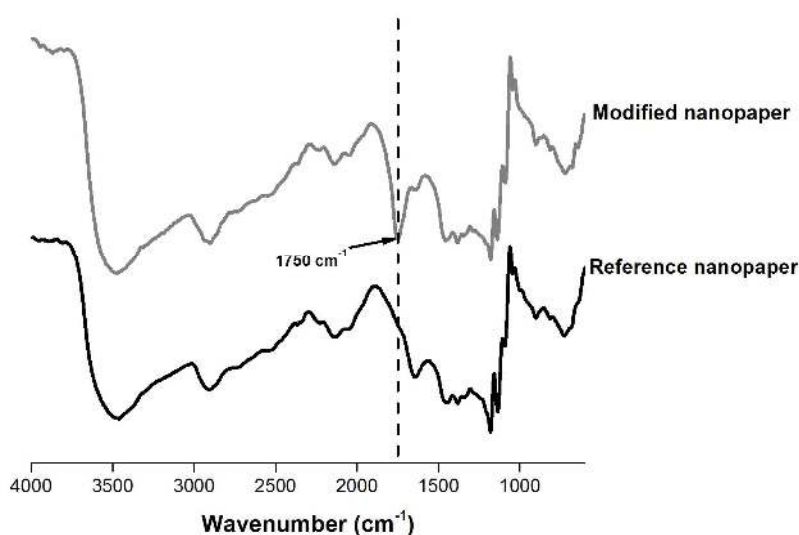
150 Dynamic mechanical analysis (DMA) under variable humidity was conducted in order to determine the
151 effect of humidity on storage modulus of reference and modified nanopaper using DMA Q800, TA
152 Instruments (New Castle, USA) (equipped with RH accessory) along with strain mode with amplitude
153 of 10 μm and frequency of 1 Hz. The samples were equilibrated at 30 $^{\circ}\text{C}$ and 0 % relative humidity for
154 2 hours to remove the absorbed moisture. Subsequently, relative humidity was raised from 0 % to 95 %
155 at the rate of 1%/min and the storage modulus was recorded. The mechanical properties in wet
156 condition were studied using same equipment and the isothermal tests were conducted in tension mode
157 at an amplitude of 20 μm and using a frequency of 1 Hz.

158 Thermogravimetric analysis (TGA) of the nanopapers (reference and modified) was conducted in order
159 to determine the thermal stability of samples using TA-TGA Q500 (New Castle, USA). Sample weight
160 around 10 mg was kept on a hanging platinum pan and heated till the temperature of 900 $^{\circ}\text{C}$ under the
161 nitrogen atmosphere, with the heating rate of 10 $^{\circ}\text{C}/\text{min}$. The moisture content of samples was
162 determined by weight loss between 0-200 $^{\circ}\text{C}$.

163 3 Results and discussion

164 3.1 Modification of CNFs

165 The esterification reaction between hydroxyl groups of CNF and carboxylic groups of LA was
166 confirmed by FTIR is shown in Figure 2. A peak around 1750 cm^{-1} (indicated by dotted line in Figure
167 2) can be seen in modified nanopaper sample, which indicates the presence of ester bond (Tjeerdsma
168 and Militz 2005). A small peak can already be observed in FTIR spectra after sonication treatment of
169 CNFs with lactic acid (see Figure 1 supplementary information). High temperature and pressure on
170 nanopapers (after water removal) was used to shift the reaction towards higher conversion.



171

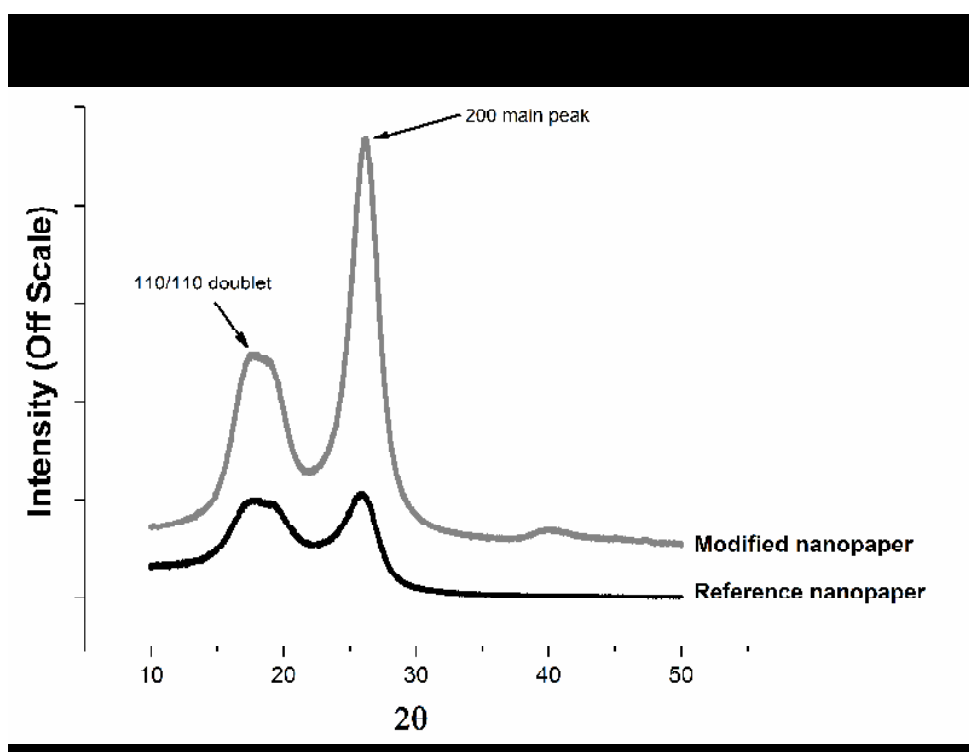
172 *Figure 2 FTIR spectra of reference and modified nanopapers. The esterification peak is marked with*
173 *dotted line around 1750 cm^{-1}*

174

175 3.2 Crystal structure

176 Effect of LA modification on crystal structure of nanopaper was studied using WAXRD and the
177 patterns of reference and modified nanopaper is shown in Figure 3. Both samples exhibited typical

178 cellulose I crystalline structure (French 2014). CrI calculated by Segal equation (Equation 1) indicated
179 different amount of crystallinity between samples (79.5% and 47.8% for modified nanopaper and
180 reference, respectively). However, from the Figure 3 it can be seen that relative heights between 1-
181 10/110 doublet and the 200 main peak varies significantly between samples. This might indicate that
182 there is substantial preferred orientation of the samples, caused by sample fabrication. The presence of
183 preferred orientation can have significant effect on the CrI calculation (Park et al. 2010). To verify this,
184 attempt to grind the samples was performed, however, due to the film-like appearance no conventional
185 grinding was successfully and intensively grinding using cryomill severely damaged the crystallinity
186 of the samples. However, based on the Scherrer equation (Equation 2), both samples exhibited similar
187 crystallite size (around 3 nm), indicating that no significant amount damage on the cellulose crystals
188 was caused by ultrasonic treatment.



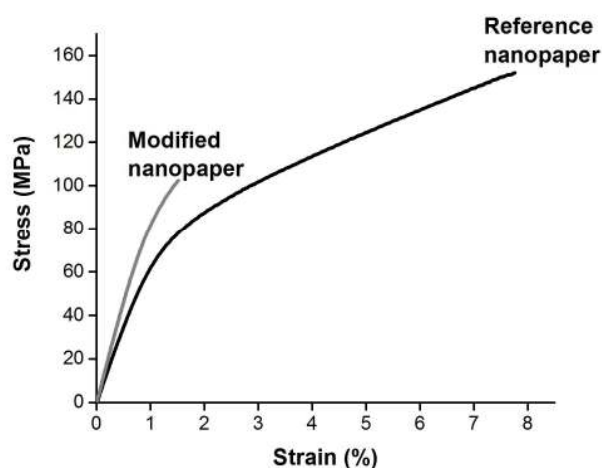
189

190

Figure 3 XRD diffraction patterns of reference and modified nanopapers.

191 3.3 Mechanical properties

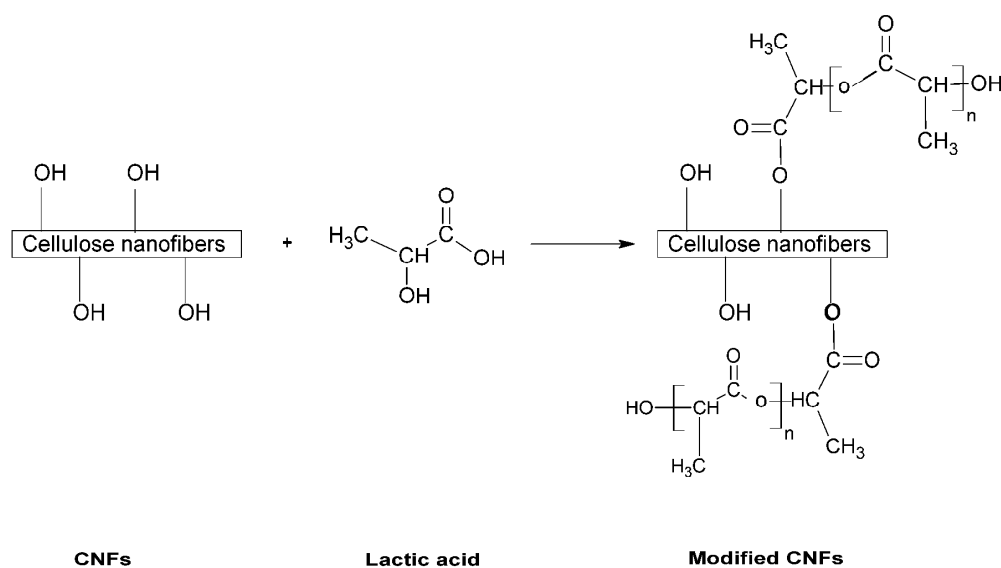
192 Compared to reference nanopaper, modified nanopaper had higher modulus (Figure 4). The increase is
193 around 32% (quantitative results are presented in Table 2). It can be speculated that the LA under the
194 high temperature of 150 °C and pressure of 10 MPa is polymerizing (or oligomerizing), as it has been
195 reported that high temperature and pressure advances the esterification reaction (Ballard et al. 1961).
196 The hydroxyl group from cellulose are also likely to participate in the reaction and forming a strong
197 covalent bond and entire structure can be considered as one rigid hybrid network where hydrogen
198 bonding of CNFs is replaced by covalent bonds, which is restricting movement of CNFs in external
199 load and hence the elastic modulus is increasing. The reaction scheme is provided in Figure 5.



200

201 *Figure 4 Stress-strain curve of reference and modified nanopaper. Modified nanopaper has higher*
202 *modulus and yield strength, and lower elongation*

203



204

205

206

207

208

209

210

211

212

213

214

215

216

217

218

219

Figure 5 Reaction scheme of CNF with LA under high pressure and temperature.

It should also be observed that the yield strength is improved in modified nanopaper by 30% (Table 2).

The strength, determined by interfibrillar sliding (Benítez et al. 2013), implies that the modified

nanopapers are more resistant to permanent deformation. This restricting of chains is clearly observed

in tensile testing fractured samples in Figure 7, where the reference nanopaper has separated fibrils at

fractured cross-section, on the other hand, in modified nanopapers the fibers are heavily bonded to each

other. The results implies that modifying the surface of CNFs can be beneficial in making stiffer

nanopapers.

The effect of sonication on cellulose was also studied. As mentioned before, sonication is an intensive

technique and provides energy of 10-100 KJ/mol (Suslick 2000; Tischer et al. 2010), which is of order

of hydrogen bonding (Tischer et al. 2010; Przybysz et al. 2016). Wang et al. concluded that sonication

can cause structural change in cellulose fibril by causing defibrillation (Wang and Cheng 2009).

Therefore, our first step was to analyze the effect of sonication by preparing a nanopaper with same

amount of sonication as modified samples. The results is presented in Table 2: the elastic modulus (E)

of sonicated nanopaper is approximately 5% less than non-sonicated one. However, it is worth

220 mentioning that the sonicated reference nanopaper has higher density (5%) so loss in modulus is more
 221 marked when density is considered.

222 Finally, the results of this study are particularly outstanding as modified nanopaper reported is 100%
 223 bio-based, offer diverse opportunities as applications such as packaging.

224

225

226

227 *Table 2 Quantitative results from stress strain analysis enlisting values (along with standard deviation)*
 228 *elastic modulus, elongation to break, tensile strength, toughness and yield strength of reference and*
 229 *modified nanopapers.*

Materials	E-modulus* (GPa)	Elongation to break* (%)	Tensile strength* (MPa)	Toughness*	Yield strength (MPa)	Density (gm/cm ³)
Reference (Unsonicated)	6.8 (0.6) ^a	8.7 (1.1) ^a	170 (18) ^a	985 (219) ^a	80 (5) ^a	1.34
Reference (Sonicated)	6.4 (0.3) ^a	11 (2.5) ^b	177 (19) ^a	1234 (360) ^a	77 (5) ^a	1.4
Modified nanopaper	9 (0.4) ^c	1.7 (0.2) ^c	111 (7) ^c	101 (24) ^c	104 (3) ^c	1.28

230 *Means that are marked by different superscript letters within the same column are significantly different at 5% level based on the one -
 231 way ANOVA.

232 3.4 Morphology

233 The reference was transparent but modified nanopaper was translucent (Figure 6); which might indicate
 234 the presence of separate phases of lactic acid and nanocellulose (Yang et al. 1996). Another possible
 235 reason can be that the modified nanopaper is porous and trapped air. The difference in density indicate
 236 the slight porosity. The reference nanopaper had density of 1.34 gm/cm³ and modified nanopaper had
 237 1.28 gm/cm³.

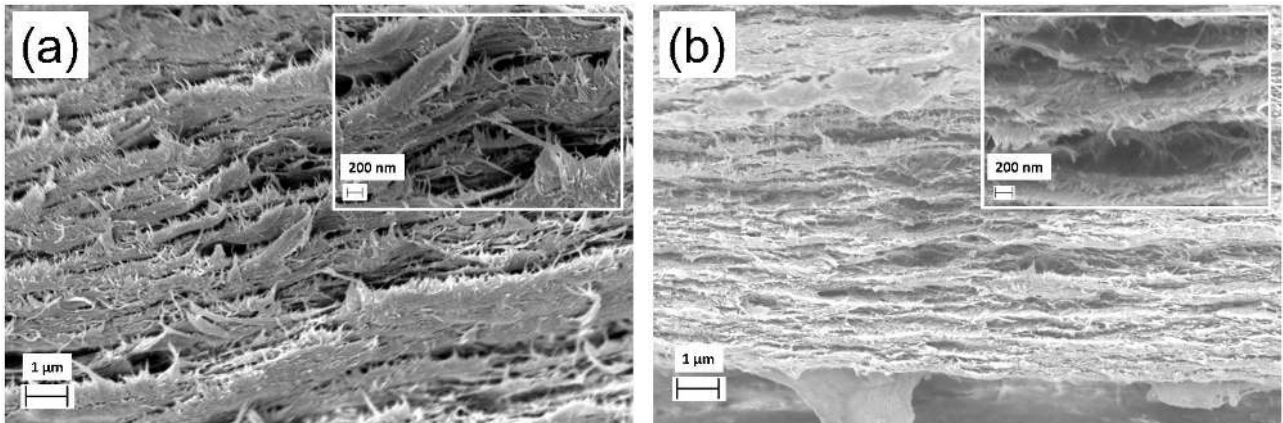


238

239

Figure 6 Photographic images of the reference nanopaper, and modified nanopaper

240



241

242

243

244

245

246

247

248

249

250

251

252

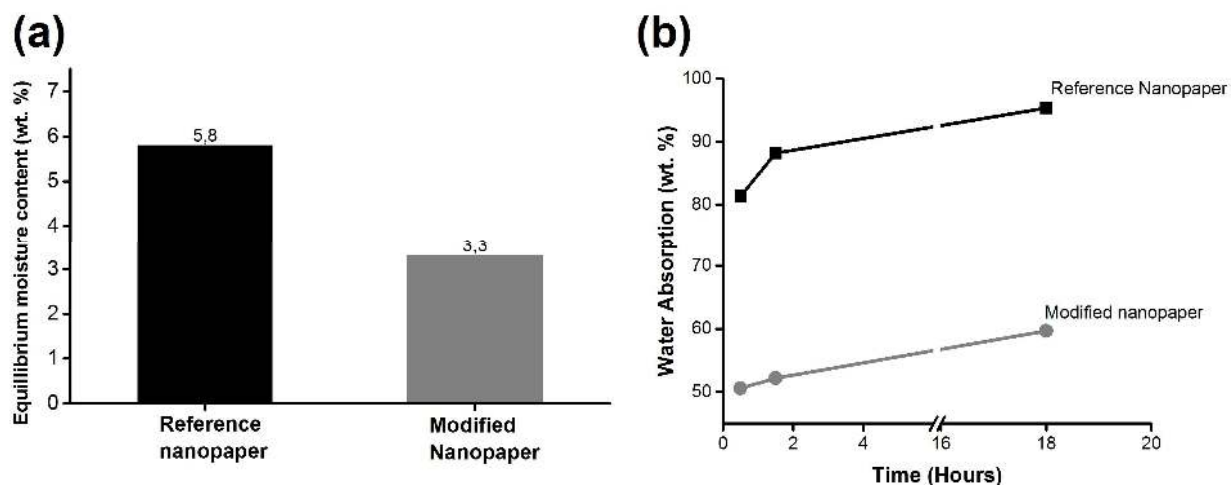
Figure 7 FESEM micrographs of fractured surface from tensile samples of (a)Reference nanopaper and (b)Modified nanopaper. Two different scales are shown: the bigger image represents the coarser scale (1μm) and inset image represents finer scale (200 nm). The reference material with typical layered structure of the nanopaper with the individual fibers. In contrast, modified nanopapers have the individual fibers and layers tightly glued to each other due to esterification.

Both reference and modified nanopaper had layered structure Figure 7 (a and b) , which is due to “concentration induced aggregation and floc formation” during filtration (Benítez et al. 2013). The reference has loosely adhered layers, indicating the debonding between the layers under the tensile load, which is likely due to breaking of inter layer hydrogen bonds. Additionally, the fracture mechanism is debonding of layers along with pull out of fibers. Small fibrils can be seen protruding from inset image of reference, no such fibrils are present in modified nanopaper. In modified

253 nanopapers, fibrils appears to be tightly glued which indicates lack of slipping. This slipping can be
254 attributed to high elongation of around 8% (Figure 7), which is missing in modified nanopaper. The
255 modified nanopaper, on the other hand, has compact structure in which layers are tightly adhered to
256 each other (Figure 7 (b)). The esterification of surface, and LA moieties are binding the layers to each
257 other which is the reason for enhanced mechanical properties (Figure 4). Additionally, the fracture
258 mechanism seems to more brittle as no fibrils are bulging from the surface (compared to reference) and
259 nanofibers are in a way glued to each other. This might be the reason for brittle fracture, as they are
260 unable to slide and fracture from cross-section instead of pull out.

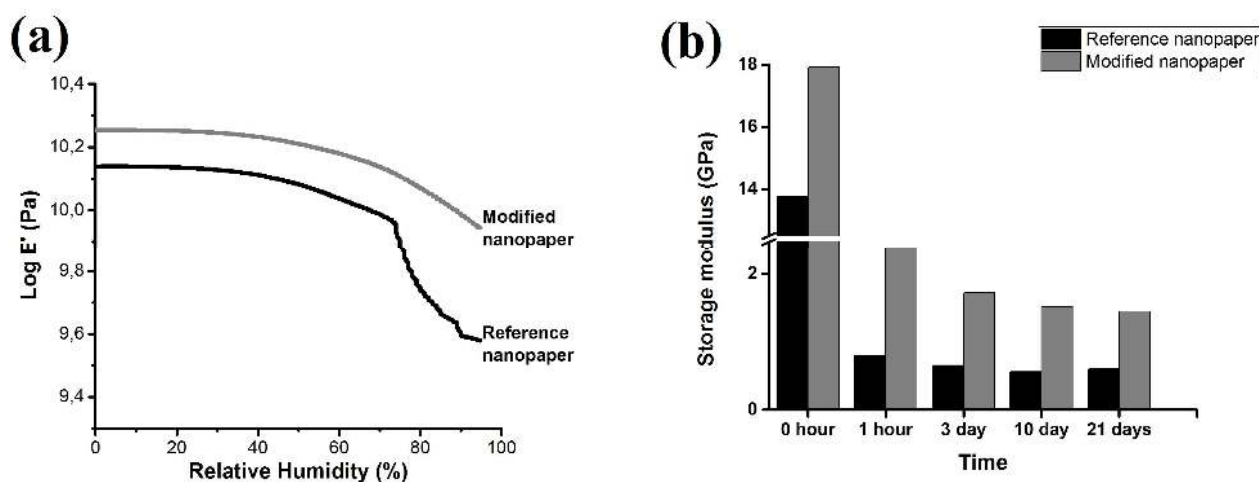
261 3.5 Effect of moisture and water content

262 The modified nanopaper was more resistant to moisture absorption from atmospheric humidity as
263 compared to nanopaper (Figure 8 (a)). It absorbed 43% less moisture compared to reference nanopaper,
264 indicating the hydrophobicity of samples. It has been mentioned that fewer hydroxyl group on the
265 surface of CNFs are accessible in the presence of polymer (oligomer) leading to lower moisture
266 absorption (Henriksson and Berglund 2007). Additionally, Figure 8 (b) presents the graph depicting
267 amount of water absorbed by samples when soaked in water. The trend is corresponding to moisture
268 content results; modified nanopaper are considerably hydrophobic than reference. The modified
269 nanopaper has 35% less water after 18 hours of absorption.



270 *Figure 8 (a) Moisture content of reference nanopaper and modified nanopapers after storing at 20 °C*
 271 *temperature and RH 50 % for 96 hours; reference has considerably high amount of moisture uptake*
 272 *than the modified nanopaper indicating the hydrophobic nature and, (b) Amount of water absorption*
 273 *as a function of time by reference nanopaper and modified nanopaper when soaked under water*

274 The modified nanopaper has better mechanical performance under humidity (Figure 9 (a)), when
 275 compared to reference nanopaper. It can be observed that humidity has devastating effect on stiffness
 276 of nanocellulose paper, which has been reported in literature (Benítez et al. 2013); however, reference
 277 nanopaper showed an interesting behavior that at relative humidity of around 75 %, it has a sharp drop
 278 in storage modulus which indicates the sample loses its stiffness suddenly. A reason might be that the
 279 water molecules are penetrating inside the material destroying the structure and acting as plasticizer,
 280 resulting in loss in storage modulus (Sehaqui et al. 2014). The results are in agreement with (Benítez et
 281 al. 2013), who also reported a steep drop in mechanical properties of nanopaper from 80 % RH to 95%
 282 RH. The modified nanopaper has higher storage modulus than reference over the entire range of
 283 humidity.



284 *Figure 9 (a) Variation of storage modulus with respect to relative humidity of modified nanopaper and*
 285 *reference nanopaper. (b) Evolution of wet storage modulus from of modified nanopaper and reference*
 286 *nanopaper, when kept in water for extended period of time*

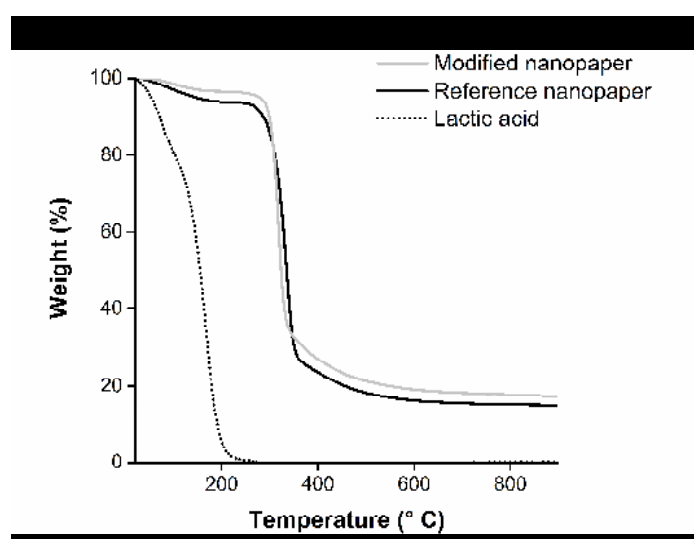
287 Figure 9 (b) presents the evolution of wet storage modulus of water soaked modified nanopaper and
 288 reference after various time intervals. It can be observed that there is a huge drop in modulus in both
 289 reference and modified nanopaper; however, the modified nanopaper have superior properties in wet
 290 state as the storage modulus is three times that of reference nanopaper even when samples are soaked
 291 in water for 21 days. The water affects the mechanical properties in two ways, by plasticizing the
 292 amorphous regions and by affecting hydrogen bonding among the nanofibrils (Benítez et al. 2013).
 293 This gives an understanding about our results. In modified nanopapers, the humidity was able to
 294 plasticize the amorphous region of cellulosic domains; however, due to presence of LA moieties at
 295 interface, it did not alleviate the bonding between fibril as it does in reference. Hence, the modified
 296 nanopaper was able to maintain higher stiffness when compared to reference. The results indicate that
 297 modified nanopaper has far better performance than reference under the influence of water.

298 3.6 Thermal stability

299 Figure 10 shows that modified nanopapers are more thermally stable than the reference nanopaper. The
 300 reference nanopaper lost 5 wt% of weight at 147 °C. On the other hand, modified nanopaper took 279

301 °C, almost twice the temperature taken by reference (90% higher) to lose 5% of weight. It is worth
302 mentioning that the results have been normalized after removing the amount of moisture in the
303 samples. Esterified nanocellulose has been reported to have better thermal stability than reference
304 (Agustin et al. 2016). It is worth noticing that at temperatures higher than 310 °C, reference has slower
305 degradation than modified samples which can be as a result from steeper degradation of LA phase.

306



307

308 *Figure 10 Thermogravimetry results indicating thermal stability of modified nanopaper along with*
309 *reference nanopaper and lactic acid; the results have been normalized after removing moisture*
310 *content. Modified nanopaper has higher stability than reference nanopape. Lactic acid thermogram is*
311 *also included.*

312 4 Conclusion

313 This study presents a novel approach to prepare modified nanopapers with enhanced properties. Lactic
314 acid monomer in aqueous medium was used, along with aid of ultrasonication and compression
315 molding. The modified nanopaper has higher modulus and yield strength, however, it lost the tensile
316 strength. Additionally, the modified nanopaper performed superiorly under humid environment and
317 presence of water. At 95% RH the storage modulus of modified nanopaper was three times that of

318 reference. Similar results were obtained for water soaked samples. Finally, the modified nanopaper was
319 thermally stable than when compared to reference nanopaper. The effect of parameters such as
320 sonication, temperature and catalyst is currently being pursued.

321 **Acknowledgements**

322 The authors acknowledge the financial support of the TEKES FiDiPro Program. Authors would also
323 like to thank Dr. Petteri Piltonen for his valuable feedback during the writing of this paper.

324 **References**

- 325 Agustin MB, Nakatsubo F, Yano H (2016) Products of low-temperature pyrolysis of nanocellulose
326 esters and implications for the mechanism of thermal stabilization. *Cellulose* 23:2887–2903. doi:
327 10.1007/s10570-016-1004-0
- 328 Ahtee M, Hattula T, Mangs J, Paakkari T (1983) An X-ray diffraction method for determination of
329 crystallinity in wood pulp. *Pap Ja Puu* 65:475–480.
- 330 Ballard CC, Broge EC, Iler RK, et al (1961) Esterification of the Surface of Amorphous Silica. *J Phys*
331 *Chem* 65:20–25. doi: 10.1021/j100819a007
- 332 Benítez AJ, Torres-Rendon J, Poutanen M, Walther A (2013) Humidity and multiscale structure govern
333 mechanical properties and deformation modes in films of native cellulose nanofibrils.
334 *Biomacromolecules* 14:4497–4506. doi: 10.1021/bm401451m
- 335 French AD (2014) Idealized powder diffraction patterns for cellulose polymorphs. *Cellulose* 21:885–
336 896. doi: 10.1007/s10570-013-0030-4
- 337 Habibi Y (2014) Key advances in the chemical modification of nanocelluloses. *Chem Soc Rev* 43:1519–
338 42. doi: 10.1039/c3cs60204d
- 339 Henriksson M, Berglund LA (2007) Structure and properties of cellulose nanocomposite films

- 340 containing melamine formaldehyde. *J Appl Polym Sci* 106:2817–2824. doi: 10.1002/app.26946
- 341 Kobayashi S, Uyama H, Suda S, Namekawa S (1997) Dehydration polymerization in aqueous medium
342 catalyzed by lipase. *Chem Lett* 26:105.
- 343 Lee K-Y, Aitomäki Y, Berglund LA, et al (2014) On the use of nanocellulose as reinforcement in polymer
344 matrix composites. *Compos Sci Technol* 105:15–27. doi: 10.1016/j.compscitech.2014.08.032
- 345 Lönnberg H, Zhou Q, Ill HB, et al (2006) Grafting of Cellulose Fibers with Poly (E -caprolactone) and
346 Poly (L -lactic acid) via Ring-Opening Polymerization. *Biomacromolecules* 7:2178–2185.
- 347 Park S, Baker JO, Himmel M E, et al (2010) Cellulose crystallinity index: measurement techniques and
348 their impact on interpreting cellulase performance. *Biotechnol Biofuels* 3:10. doi: 10.1186/1754-
349 6834-3-10
- 350 Peltzer M, Pei A, Zhou Q, et al (2014) Surface modification of cellulose nanocrystals by grafting with
351 poly(lactic acid). *Polym Int* 63:1056–1062. doi: 10.1002/pi.4610
- 352 Przybysz P, Dubowik M, Kucner M A, et al (2016) Contribution of Hydrogen Bonds to Paper Strength
353 Properties. *PLoS One* 11:e0155809.
- 354 Sehaqui H, Ezekiel Mushi N, Morimune S, et al (2012) Cellulose nanofiber orientation in nanopaper
355 and nanocomposites by cold drawing. *ACS Appl Mater Interfaces* 4:1043–1049. doi:
356 10.1021/am2016766
- 357 Sehaqui H, Zimmermann T, Tingaut P (2014) Hydrophobic cellulose nanopaper through a mild
358 esterification procedure. *Cellulose* 21:367–382. doi: 10.1007/s10570-013-0110-5
- 359 Suslick KS (2000) Sonochemistry. In: *Kirk-Othmer Encyclopedia of Chemical Technology*. John Wiley &
360 Sons, Inc.,
- 361 Tanaka H, Kurihashi T (2003) Synthesis of Polyesters by Emulsion Polycondensation Reaction in Water.

362 Polym J35:359–363. doi: 10.1295/polymj.35.359

363 Teramoto Y, Yoshioka M, Shiraishi N, Nishio Y (2002) Plasticization of cellulose diacetate by graft
364 copolymerization of ϵ -caprolactone and lactic acid. *J Appl Polym Sci* 84:2621–2628. doi:

365 10.1002/app.10430

366 Tingaut P, Zimmermann T, Sèbe G (2012) Cellulose nanocrystals and microfibrillated cellulose as
367 building blocks for the design of hierarchical functional materials. *J Mater Chem* 22:20105. doi:

368 10.1039/c2jm32956e

369 Tischer PCSF, Sierakowski MR, Westfahl H, Tischer CA (2010) Nanostructural reorganization of
370 bacterial cellulose by ultrasonic treatment. *Biomacromolecules* 11:1217–1224. doi:

371 10.1021/bm901383a

372 Tjeerdsma BF, Militz H (2005) Chemical changes in hydrothermal treated wood: FTIR analysis of
373 combined hydrothermal and dry heat-treated wood. *Holz als Roh - und Werkst* 63:102–111. doi:

374 10.1007/s00107-004-0532-8

375 Wang S, Cheng Q (2009) A novel process to isolate fibrils from cellulose fibers by high-intensity
376 ultrasonication, Part 1: Process optimization. *J Appl Polym Sci* 113:1270–1275. doi:

377 10.1002/app.30072

378 Yang J, Winnik MA, Yitalo D, Devoe RJ (1996) Polyurethane-Polyacrylate Interpenetrating Networks.
379 1. Preparation and Morphology. *Macromolecules* 9297:7047–7054. doi: 10.1021/ma9601373

380 Yoo DK, Kim D, Lee DS (2006) Synthesis of lactide from oligomeric PLA: Effects of temperature,
381 pressure, and catalyst. *Macromol Res* 14:510–516. doi: 10.1007/BF03218717

382 8